

# Simple Methods for Estimating Backwater and Constriction Scour at Bridges and Abrupt Encroachments

STEWART W. TAYLOR AND HSIEH WEN SHEN

Analytic expressions for bridge backwater and constriction scour are presented for subcritical flow through five commonly occurring bridge crossings. To assess the effects of constriction scour on bridge backwater, a known cross-section technique is employed. Based on the analytic expressions, bridge backwater and constriction scour are numerically simulated over a wide range of flow conditions. Regression analysis is used to develop simplified explicit relations for bridge backwater as a function of Froude number, pier energy-loss coefficient, constriction ratio, and conveyance ratio. The resulting regression equations are sufficiently accurate for preliminary hydraulic analyses of bridge waterways in a feasibility study. Simplified expressions are not intended for detailed design analysis. Practical application of the simplified expressions is illustrated through a step-by-step design procedure.

In a feasibility or preliminary design phase of a bridge, highway engineers are faced with estimating bridge backwater, scour of the bridge waterway, and the effects of scour on the bridge backwater. Extensive literature has been written on these subjects; many rigorous methods are available for detailed analysis. The existing methods or models often require access to a computer and a large amount of detailed data, such as river channel geometry, sediment data, geometry of the bridge, and so forth. At the feasibility or preliminary level, detailed data are often nonexistent and often estimated; hence, a detailed analysis is not justified in terms of accuracy or in the time required for the lengthy computations. Highway engineers must explore many options in the feasibility or preliminary phase. A simple yet reasonably accurate hydraulic analysis, given the data constraints, is presented here and is intended to guide highway engineers' decision making before a detailed analysis is made. The advantages of this analysis over other short-cut methods are as follows: (a) bridge backwater is functionally related to easily computed uniform-flow properties and bridge characteristics; and (b) bridge backwater is computed explicitly, whereas other procedures involve a trial solution.

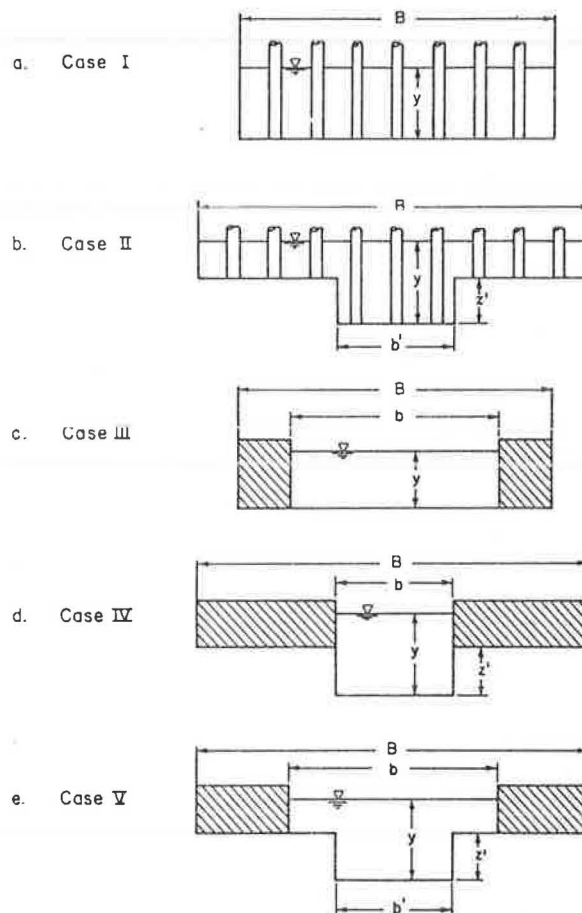
## ANALYSIS OF BACKWATER AND CONSTRICTION SCOUR

Simple methods are based on the detailed analysis of flow modification by bridges and abrupt encroachments presented by Taylor (1); highlights are given below. Bridge crossings are grouped into five categories, shown in Figure 1, and are described as follows: case I, bridge piers crossing a river channel; case II, bridge piers crossing a river channel with floodplains; case III, abrupt width encroachment of a river channel; case IV, total abrupt encroachment of floodplains; and case V, partial abrupt encroachment of floodplains. These five cases were selected to represent commonly occurring bridge crossings. Additional cases could be created by introducing bridge piers in the width encroachment; our studies, however, indicate that additional backwater caused by piers in such cases is small when compared with the magnitude of the backwater due to width encroachment.

### Assumptions

Some assumptions are made to generalize and simplify the analysis with the knowledge that only rough estimates are obtainable from simple solutions.

Figure 1. Nomenclature.



1. Flow is subcritical.

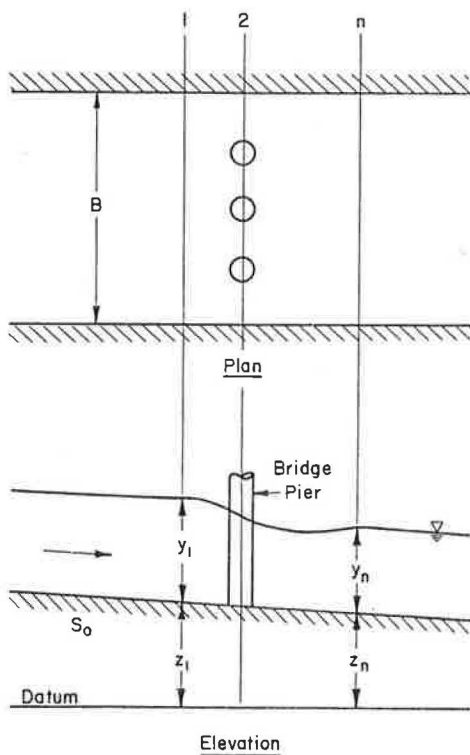
2. Bridge crossings are normal to the flow (non-skew), and floodplains are symmetrical around the river channel (noneccentric). Although bridge openings are often skew or eccentric in practice, introducing these variables, given the degree to which the flood discharge, channel roughness, and so on are known, defeats the whole purpose of a simple analysis.

3. Flow never overtops the lowest elevation of the encroachment embankment (no weir flow) and never contacts the bottom of the bridge deck (no orifice flow); occurrence of either of these phenomena could cause a bridge failure. This study assumes that sufficient freeboard will be incorporated into the bridge design to prevent weir flow or orifice flow.

4. Flow is uniform before the construction of a bridge crossing; i.e., flow at the future bridge site is not strongly influenced by some downstream control. Uniform-flow conditions are easily calculated and are useful parameters on which simple solutions may be based.

5. Constriction scour occurs uniformly within

Figure 2. Definition sketch for bridge piers: cases I and II.



the bridge opening, and local scour is neglected. Without detailed knowledge of sediment sizes and the lateral distribution of bed shear stress, it is not possible to predict the lateral distribution of constriction scour. Local scour around piers may be estimated from any of the numerous pier-scour equations and superimposed onto the constriction scour depth to estimate the total depth of scour.

6. There is no change in river regime; i.e., the river is quasi-stable from a geomorphic point of view. Potential changes in the river regime should be studied once the final bridge site has been chosen and more data are available.

#### Backwater Analysis

The steady-state backwater, or increase in stage upstream from a bridge crossing, is found by applying the energy equation across the control volumes shown in Figures 2 and 3. For valid application of the one-dimensional energy equation, control volumes are selected so that the flow at a given cross section is nearly one-dimensional in the longitudinal direction and the pressure distribution is nearly hydrostatic in the vertical direction.

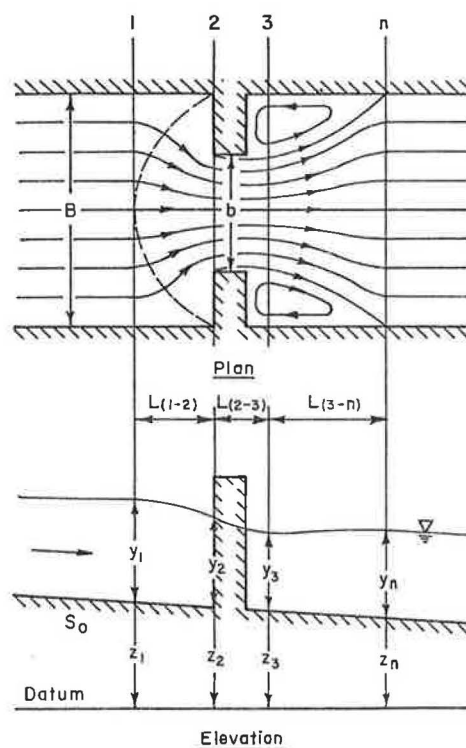
With reference to Figure 2, the backwater for the bridge piers of cases I and II is found by considering the energy balance between sections 1 and n. For uniform flow without bridge piers, flow velocity and depth are by definition constant in the longitudinal direction. The energy equation for uniform flow may be written as follows:

$$\alpha_n (U_n^2/2g) + y_n + z_n = \alpha_n (U_n^2/2g) + y_n + z_n + h_{f(1-n)} \quad (1)$$

where

$\alpha$  = kinetic energy coefficient,  
 $U$  = mean flow velocity,  
 $g$  = acceleration of gravity,

Figure 3. Definition sketch for abrupt encroachment: cases III, IV, and V.



$y$  = flow depth,  
 $z$  = bed elevation, and  
 $h_{f(1-n)}$  = energy loss due to friction.

With bridge piers the energy balance is expressed as follows:

$$\alpha_1 (U_1^2/2g) + y_1 + z_1 = \alpha_n (U_n^2/2g) + y_n + z_n + h'_{f(1-n)} + h_{L(1-n)} \quad (2)$$

where the energy loss due to piers is assumed to be of the form

$$h_{L(1-n)} = K_L \alpha_n (U_n^2/2g) \quad (3)$$

Subtracting Equation 1 from Equation 2 and rearranging yields

$$y_1 - y_n = \alpha_n (1 + K_L) (U_n^2/2g) - \alpha_1 (U_1^2/2g) + h'_{f(1-n)} - h_{f(1-n)} \quad (4)$$

The upstream velocity  $U_1$  may be written in terms of  $U_n$  by using the relation for mass conservation,

$$Q = A_1 U_1 = A_n U_n \quad (5)$$

Because the friction losses with and without bridge piers are approximately equal, i.e.,  $h'_{f(1-n)} = h_{f(1-n)}$ , Equation 4 becomes

$$y_1 - y_n = [\alpha_n (1 + K_L) - \alpha_1 (A_n/A_1)^2] (U_n^2/2g) \quad (6)$$

Dividing by the normal hydraulic depth ( $A_n/B$ , where  $B$  is the channel top width) results in the nondimensional backwater expression

$$y^*/(A_n/B) = 1/2 [\alpha_n (1 + K_L) - \alpha_1 (A_n/A_1)^2] F_n^2 \quad (7)$$

where  $F_n = U_n/(gA_n/B)^{1/2}$  is the Froude number and  $y^* = y_1 - y_n$  is the backwater. The pier energy-loss coefficient ( $K_L$ ) is generally a function of the pier shape and degree of pier constric-

tion. As an approximation, the  $\Delta K_D$  of Bradley (2), which is equivalent to  $K_L$ , may be used to evaluate  $K_r$ . Equation 7 requires a trial-and-error solution for  $y_1$  that is easily computed in three to four iterations by using the Newton-Raphson convergence scheme once  $A_1$  and  $\alpha_1$  are in terms of  $y_1$ .

Backwater associated with the abrupt encroachments of cases III, IV, and V is found by applying the energy equation in a stepwise fashion to the control volumes shown in Figure 3. Given the downstream boundary condition  $y_n$ , the energy equation is applied between section  $n$  and section 3, where flow depth is a minimum, to solve for  $y_3$ . Data of Liu, Bradley, and Plate (3) indicate that section 3 roughly coincides with the downstream face of the embankment. Once  $y_3$  has been determined, the energy equation is written from section 3 to section 1 and solved for  $y_1$ . The two energy expressions are thus

$$\alpha_3 (U_3^2/2g) + y_3 + z_3 = \alpha_n (U_n^2/2g) + y_n + z_n + h_{f(3-n)} + h_{L(3-n)} \quad (8)$$

$$\alpha_1 (U_1^2/2g) + y_1 + z_1 = \alpha_3 (U_3^2/2g) + y_3 + z_3 + h_{f(1-3)} \quad (9)$$

where

- $h_{f(3-n)}$  = friction loss occurring in the control volume bounded by sections 3 and  $n$ ,
- $h_{L(3-n)}$  = eddy loss occurring in the control volume bounded by sections 3 and  $n$ , and
- $h_{f(1-3)}$  = friction loss occurring in the control volume bounded by sections 1 and 3.

Schneider and others (4) define the friction losses as follows:

$$h_{f(3-n)} = L_{(3-n)} Q^2 / K_3 K_4 \quad (10)$$

$$h_{f(1-3)} = [L_{(1-2)} Q^2 / K_1 K_3] + [L_{(2-3)} Q^2 / K_3^2] \quad (11)$$

where  $K$  is the conveyance. Reach lengths  $L_{(1-2)}$ ,  $L_{(2-3)}$ , and  $L_{(3-n)}$  are determined as follows. The accelerating flow upstream from the abrupt encroachment may be studied by using potential-flow analysis. Figure 3 shows the streamlines that result from a Schwarz-Christoffel transformation of a potential source in a half-plane with boundaries representing those in open channel flow. Schneider and others (4) locate section 1 of the intersection of the center streamline and the equipotential line emanating from the points where the water edge and embankments intersect. Section 2 is located at the upstream face of the embankment. As demonstrated by Schneider and others (4), the straight-line distance between sections 1 and 2 is not representative of the average streamline length. Instead, the lengths of all streamlines are averaged to find  $L_{(1-2)}$  as a function of the straight-line distance and the constriction ratio. The length  $L_{(2-3)}$  is approximately the length of the abrupt encroachment, simply the bridge embankment width. As seen in Figure 3, the reach between sections 3 and  $n$  is characterized by large eddies downstream from the encroachment that result from flow separation occurring at or slightly upstream from section 3. The length of the separation zone, approximately  $L_{(3-n)}$ , is the distance from the efflux of the abrupt expansion to the point where flow reattaches to the sidewalls of the channel. For case III, measurements by Abbott and Kline (5) are used to estimate  $L_{(3-n)}$  as a function of the area ratio. Field observations by Schneider and others (4) suggest that  $L_{(3-n)}$  is one encroachment width  $b$  for cases IV and V.

Energy loss due to lateral mixing in the expansion reach is given by Taylor (1) as follows:

$$h_{L(3-n)} = K_L (H/b) (U_3^2/2g) \quad (12)$$

where  $H = (B - b)/2$ , the step height. For case III,  $K_L$  is obtained by numerically integrating velocity-profile data for abrupt channel expansions, given by Lokrou (6). The relation between  $K_L$  and the constriction ratio  $\sigma = b/B$  is shown in Figure 4 (6). A different relation for  $K_L$  is derived for cases IV and V based on the observed field data of Schneider and others (4); it is given in Figure 5.

With all energy-loss terms defined, Equation 8 is solved by trial and error for  $y_3$ ; Equation 9 is then solved by trial and error for  $y_1$  given  $y_3$ . A Newton-Raphson convergence scheme may be used to speed computations.

### Constriction Scour

The constriction scour resulting from bridge piers, cases I and II, was found to be negligibly small when compared with local scour. By using a physical model study, Laursen and Toch (7) found that the effect of pier contraction on scour will seldom be important in modern bridge design. They indicated that in order for the depth of scour to be appreciably affected, the contraction would have to be about 10 percent, an amount seldom attained in current bridge design practice. Although constriction scour is small for bridge piers, local scour may be substantial. The mechanics of local scour around piers has been discussed by Shen (8) and by Richardson and others (9).

Constriction scour for cases III, IV, and V is estimated by considering the equilibrium scour depth in a long constriction. The constriction-scour depth ( $\Delta y_s$ ), shown in Figure 6, is found by

Figure 4. Coefficient of energy loss due to lateral mixing: case III.

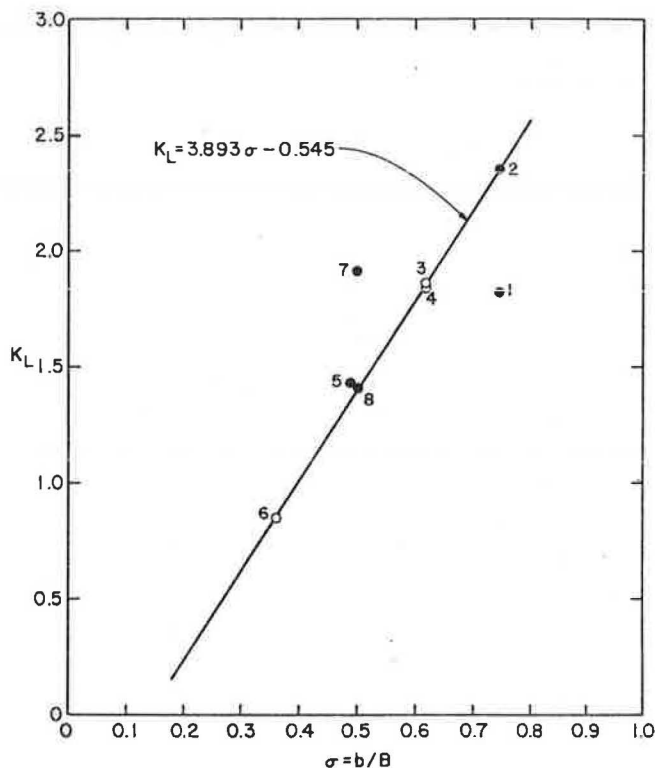


Figure 5. Coefficient of energy loss due to lateral mixing: cases IV and V.

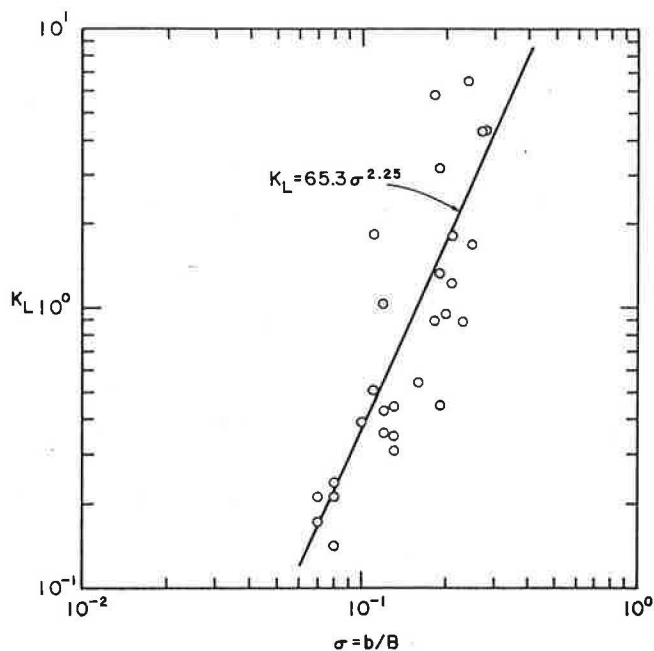
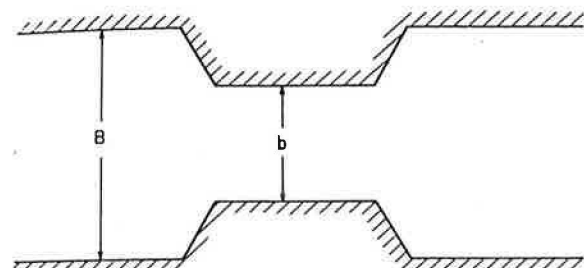
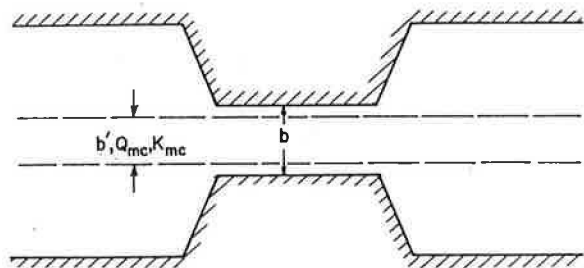


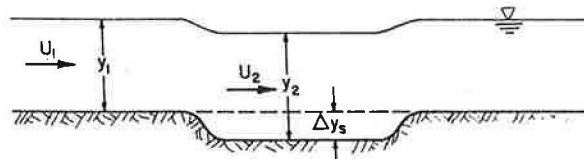
Figure 6. Definition sketches for constriction scour.



a. Plan View - Cases I, II and III

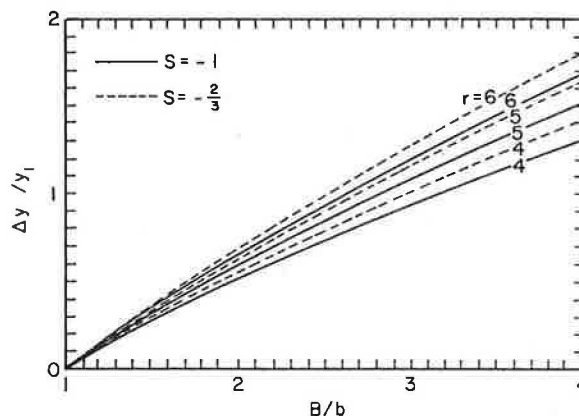


b. Plan View - Cases IV and V



c. Profile View

Figure 7. Constriction scour: case III.



solving the equations of water continuity, sediment continuity, and sediment transport simultaneously. When the sediment transport into the constriction is the same as the transport out of the constriction, the scour hole achieves the dynamic equilibrium

$$Q_s = q_{s1} B = q_{s2} b \quad (13)$$

where  $Q_s$  is the sediment discharge and  $q_s$  is the sediment discharge per unit width.

For case III, a simple sediment transport function is chosen:

$$q_s = K U^r y^s \quad (14)$$

where  $K$  is an empirical coefficient, and the exponent  $r > 0$  and  $s < 0$ . Laursen (10) has shown that the bed-load equations of Dubois, Shields, Schoklitsch, Meyer-Peter and Muller, and Brown-Einstein can be reduced to Equation 14. The coefficient  $K$  is generally a function of channel characteristics, channel roughness, and bed-material size. The exponent  $r$  ranges between 4 and 6, whereas the exponent  $s$  varies between  $-2/3$  and  $-1$ . Solving Equations 5, 13, and 14 simultaneously and letting  $\Delta y_s = y_2 - y_1$  gives

$$\Delta y_s / y_1 = (B/b)^{(1-r)/(s-r)} - 1 \quad (15)$$

Equation 15 is plotted in Figure 7 for  $r = 4, 5, 6$ , and  $s = -2/3, -1$ . In the absence of better data, choosing  $r = 6$  and  $s = -2/3$  will give a conservative estimate of constriction scour.

Constriction scour for cases IV and V is found by using the analysis by Laursen (11). Assuming that no sediment is transported over the floodplains, the Manning resistance equation, the water and sediment continuity equations, and the sediment transport relation given by Laursen (12) may be solved simultaneously to give

$$y_2 / y_1 = (Q / Q_{mc})^{6/7} (b' / b)^{6/7 [(2+a)/(3+a)]} (n_2 / n_1)^{6/7 [a/(3+a)]} \quad (16)$$

where  $Q_{mc}$  is the discharge conveyed in the main channel,  $b'$  is the main-channel width, and  $a$  is the exponent depending on the ratio of shear velocity to fall velocity ( $u_* / w$ ). Laursen's analysis (11) suggests that the maximum scour depths occur for large values of  $u_* / w$ . Assuming  $a = 9/4$  ( $u_* / w > 2$ ),  $n_1 = n_2$ , and  $Q / Q_{mc} = K / K_{mc}$ , Equation 16 may be written

$$\Delta y_s / y_1 = (K / K_{mc})^{0.86} (b' / b)^{0.69} - 1 \quad (17)$$

Negative values of  $\Delta y_s/y_1$  may be obtained from Equation 17 but have no physical meaning. If negative values are computed, it is assumed that  $\Delta y_s = 0$ . For case IV,  $b'/b = 1$  so that

$$\Delta y_s/y_1 = (K/K_{mc})^{0.86} - 1 \quad (18)$$

Equations 17 and 18 are plotted in Figure 8.

#### Effects of Constriction Scour on Backwater

Constriction scour enlarges the bridge opening, which in turn relieves or reduces the backwater. Although the development of scour is a time-dependent process, the backwater in such a case may be estimated by assuming that the scour develops instantly. This is reasonable, because the time required for the constriction scour hole to achieve its full equilibrium depth is short, probably less than an hour for a sand-bed stream. To assess the effect of scour on backwater, the backwater is first computed based on the preceding energy analysis for the case of no scour, i.e., a rigid boundary assumption. The depth of constriction scour ( $\Delta y_s$ ) is estimated from the appropriate scour relation—Equation 15, 17, or 18—and is subtracted from  $z_3$  to obtain the elevation of the scoured bed. Backwater is then recomputed for the fully scoured condition. This procedure is termed the known cross-section method. The difference  $y^* - y_s^*$ , where  $y_s^*$  is the backwater associated with constriction scour, reflects the amount that the backwater has been reduced by the scour.

#### SIMPLE METHODS FOR ESTIMATING BACKWATER

The backwater equations presented in the previous section, with or without constriction scour, require an iterative solution for  $y^*$  or  $y_s^*$ , which makes them impractical for quick, preliminary estimates of backwater. To avoid the trial-and-error procedure inherent in this or any other bridge backwater analysis, the backwater equations are formulated into an iterative computer model, which is used to synthesize a large data base. The synthesized backwater data, generated over a wide range of flow conditions and channel constrictions, are nondimensionalized. Regression analysis is used to fit a model from which backwater may be determined explic-

itly. Although the regression model may not be able to reproduce the results from the analytic expression exactly, the approximate nature and need for quick backwater estimates at the feasibility study level justify the approach.

#### Dimensional Analysis

Grouping variables nondimensionally into physically meaningful parameters is a useful way of reducing the number of independent variables describing bridge backwater. The analysis of backwater and constriction scour indicates that the general relation (cases I-V) for backwater is of the form

$$y^* = f(\alpha_n, Q, A_n, g, b, B, K, K_{mc}, K_L, n_{ob}, n_{mc}, \Delta y_s) \quad (19)$$

where  $n_{ob}$  is the overbank and  $n_{mc}$  is the main-channel Manning roughness coefficient. By inspection, Equation 19 is nondimensionalized to give

$$y^*/y_n = f[\alpha_n, Q/(g A_n^3/B)^{1/2}, b/B, K_{mc}/K, K_L, n_{mc}/n_{ob}, \Delta y_s/y_n] \quad (20)$$

in which

$$F_n = Q/(g A_n^3/B)^{1/2} \quad (21)$$

is recognized as the Froude number.

#### Regression Analysis

The synthesized data base was nondimensionalized according to Equation 20 and transformed into logarithms. Stepwise (forward) regression analyses of the transformed data were made based on the following criteria: F-level for inclusion = 0.01; F-level for deletion = 0.005; and tolerance level = 0.001. Results of the regression analysis, including regression statistics of the transformed data, are given in Figures 9-16. For the sake of brevity, the extensive plotted results of case IV, rigid boundary, are not included. The complete results are discussed elsewhere (1). The regression equations may be easily solved for backwater by using a hand-held calculator, or if a graphical solution is desired, the figures may be used directly. The range of flow conditions, channel properties, and bridge opening widths for the data base is summarized in Figure 17. For the rigid boundary condition of case III (Figure 12), laboratory data of Liu, Bradley, and Plate (3) were used in the analysis rather than synthesized data.

#### Discussion of Results

For the bridge piers of case I, the regression analysis indicated that the backwater ratio is a function of  $F_n$  and  $K_L$  only. For the case II bridge piers, regression analysis indicated that the product  $(\alpha_n)^{1/2} F_n$  and  $K_L$  describe the backwater ratio in nonuniform channels. The influence of pier width and spacing and pier shape is absorbed into the loss coefficient  $K_L$ . Because constriction scour was shown to be negligible for bridge piers, the results are applicable to both rigid- and movable-boundary conditions.

Laboratory data (simple normal crossing, vertical board abrupt encroachment) of Liu, Bradley, and Plate (3) were used in the case III rigid-boundary regression analysis. By combining  $F_n$  and  $b/B$  into one term, the backwater was found to be a function of a single parameter. Because  $K_L$  is a linear function of  $b/B$  (Figure 4), energy losses in terms of  $K_L$  are contained implicitly in the denominator of  $F_n/(b/B)$ . For case III, movable-boundary backwater data were numerically simulated. The regres-

Figure 8. Constriction scour: cases IV and V.

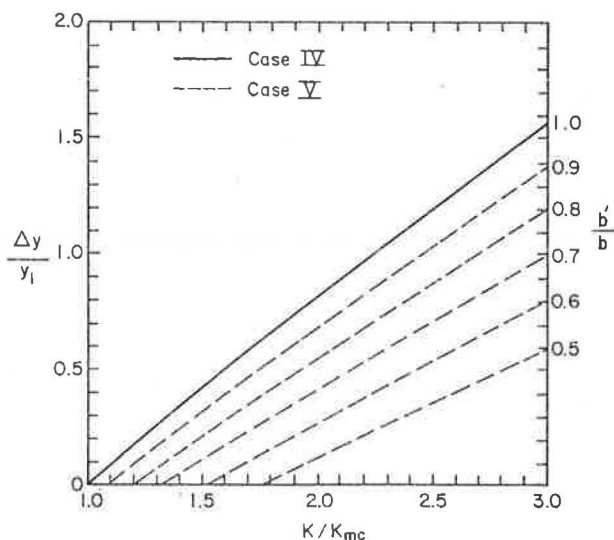




Figure 9. Results of regression analysis.

Case	Boundary Type	Equation	N	R <sup>2</sup>	S	Error
I	Rigid or Movable	$\frac{y^*}{y_n} = F_n^{[3.300 + \log F_n (1.281 + 0.406 \log F_n)]} K_L^{0.974}$	(22) 120	0.99	0.014	±3%
II	Rigid or Movable	$\frac{y^*}{A/B} = 0.815 (\sqrt{\alpha_n F_n})^X K_L^{0.615}$ $X = 2.434 + 0.223 \log \sqrt{\alpha_n F_n} + \log K_L (-1.152 - 0.759 \log \sqrt{\alpha_n F_n})$	(23) 189	0.99	0.026	±6%
III	Rigid	$\frac{y^*}{y_n} = 0.661 \left( \frac{F_n}{b/B} \right)^{2.064}$	(25) 57	0.94	N/A	
	Movable	$\frac{y^*}{y_n} = 0.181 \left( \frac{F_n}{b/B} \right)^{2.208}$	(26) 360	0.98	0.090	-19%, +23%
IV	Rigid	$\frac{y^*}{y_n} = 1.123 F_n^{1.871} \left( \frac{K_{mc}}{K} \right)^{-3.116} \left( \frac{b'}{B} \right)^{0.553} \left( \frac{n_{mc}}{n_{ob}} \right)^{-0.805}$	(27) 225	0.96	0.16	-31%, +45%
	Movable	$\frac{y^*}{y_n} = 1.173 F_n^{1.148} \left( \frac{y^*}{y_n} \right)^{0.413}$	(28) 225	0.97	0.13	-26%, +35%
V	Rigid	$\frac{y^*}{y_n} = 1.123 F_n^{1.871} \left( \frac{K_{mc}}{K} \right)^{-3.116} \left( \frac{b'}{B} \right)^{0.553} \left( \frac{n_{mc}}{n_{ob}} \right)^{-0.805}$	(29) 675	—	—	
	Movable	$\frac{y^*}{y_n} = 1.218 F_n^{0.795} \left( \frac{y^*}{y_n} \right)^{0.566}$	(30) 675	0.97	0.15	-29%, +41%

N = number of samples  
R<sup>2</sup> = coefficient of determination  
S = standard error of estimate  
Error: 2/3 of the data fell within this error range

sion analysis indicated that the movable-boundary backwater could also be expressed as a function of the single variable  $F_n/(b/B)$ . The constriction scour depth ( $\Delta y_s$ ) is included implicitly in  $b/B$ , as suggested by Equation 15. Although exponents  $r$  and  $s$  were varied in the simulation ( $4 < r < 6$  and  $-2/3 < s < -1$ ), the backwater was found to be insensitive to these parameters. An expression relating the movable-boundary backwater to the rigid-boundary backwater is found by dividing Equation 25 by Equation 24, or

$$y_s^*/y_n^* = 0.274 [F_n/(b/B)]^{0.144} \quad (30)$$

This relation indicates the degree to which constriction scour will relieve the backwater from the rigid-boundary condition.

Backwater for case IV, rigid boundary, was found to be a function of four variables, as given by Equation 26. Stepwise regression showed that  $F_n$  and  $K_{mc}/K$  accounted for 95 percent of the variation in  $y^*/y_n$ , although  $b/B$  and  $n_{mc}/n_{ob}$  were significant at an F-level for inclusion of 0.01. The standard error of the estimate ( $S = 0.16$ ) suggests that the error associated with Equation 26 is -31 to +45 percent. The kinetic energy correction factor ( $\alpha_n$ ) was not found to be a significant parameter, even though  $\alpha_n$  varied over a wide range ( $1 < \alpha_n < 9$ ). A simple model for case IV, movable boundary, was developed by relating the movable-boundary backwater to the rigid-boundary backwater so that  $y_s^*/y_n = f(F_n, y^*/y_n)$ . Constriction scour ( $\Delta y_s$ ) as given by Equation 18 is a function of  $K_{mc}/K$  and is thus contained implicitly in  $y^*/y_n$ . The standard error of the estimate ( $S = 0.13$ ) suggests that the absolute error in using the movable-boundary relation (Equation 27) is -26 percent, +35 percent. A more accurate estimate of the movable-boundary backwater may be obtained from

$$y_s^*/y_n = 8.93 F_n^{1.93} (\Delta y_s/y_n)^{0.650} (b/B)^{0.921} (n_{mc}/n_{ob})^{-1.06} \quad (31)$$

in which  $R^2 = 0.99$  and  $S = 0.061$ ; the absolute error

is -13 to +15 percent. For the sake of brevity, no graphical solution of Equation 31 is given.

For the range of conditions investigated, the backwater for the partial floodplain encroachment case V, rigid boundary, was found to be of the same order as that for case IV. A comparison of the case V backwater against case IV backwater is shown in Figure 16. Evidently the backwater is nearly the same for both cases over the investigated range of  $b'/b$ , although the expected decreasing trend for case V is somewhat apparent. More data are required to assess the flow distribution and energy losses for case V, because Figure 16 indicates that in some instances the backwater for case V is greater than that for case IV, a physical impossibility. For practical purposes, however, the rigid-boundary backwater of case V may be conservatively evaluated by using the relation for case IV. The movable-boundary backwater relation for case V is similar to that developed for case IV, i.e.,  $y_s^*/y_n = f(F_n, y^*/y_n)$ , although the numerical constants differ in magnitude. The standard error of the estimate ( $S = 0.15$ ) suggests that the absolute error in using the movable-boundary backwater relation (Equation 29) is -29 percent, +41 percent.

#### PRACTICAL APPLICATION

Practical application of the simplified backwater and constriction scour relations is demonstrated as follows:

Step 1: Estimate the uniform-flow conditions of the river reach under consideration for the design discharge. If a rating curve does not exist, the Manning equation may be used to derive the rating curve. Cross-sectional area, wetted perimeter, and top width may be tabulated from river cross sections. The river slope may be computed from river cross sections or topographic maps. Studies by Chow (13) and Barnes (14) are useful references for estimating Manning  $n$ -values.

Step 2: After the river configuration has been studied, use Figure 1 to categorize the river cross-sectioning as case I, case II, and so on. Enter Figure 9

Figure 10. Change in water-surface elevation: case I, rigid boundary.

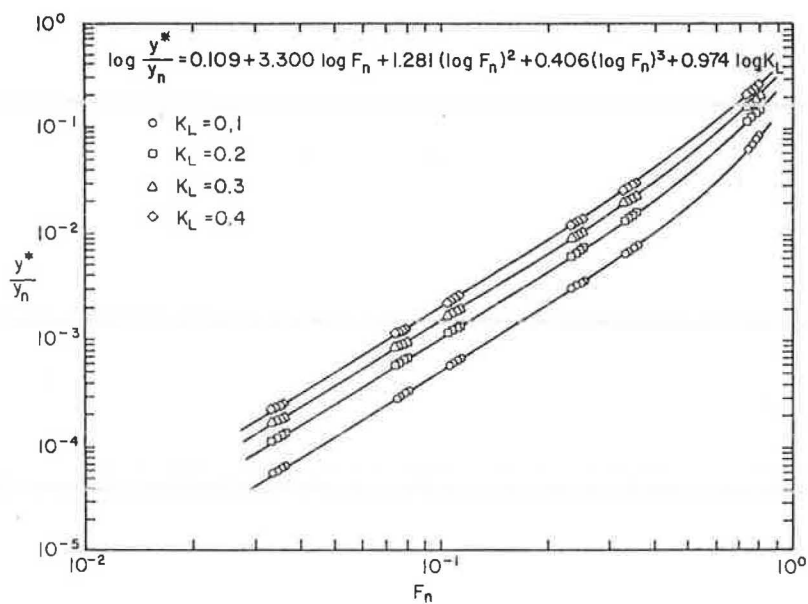


Figure 11. Change in water-surface elevation: case II, rigid boundary.

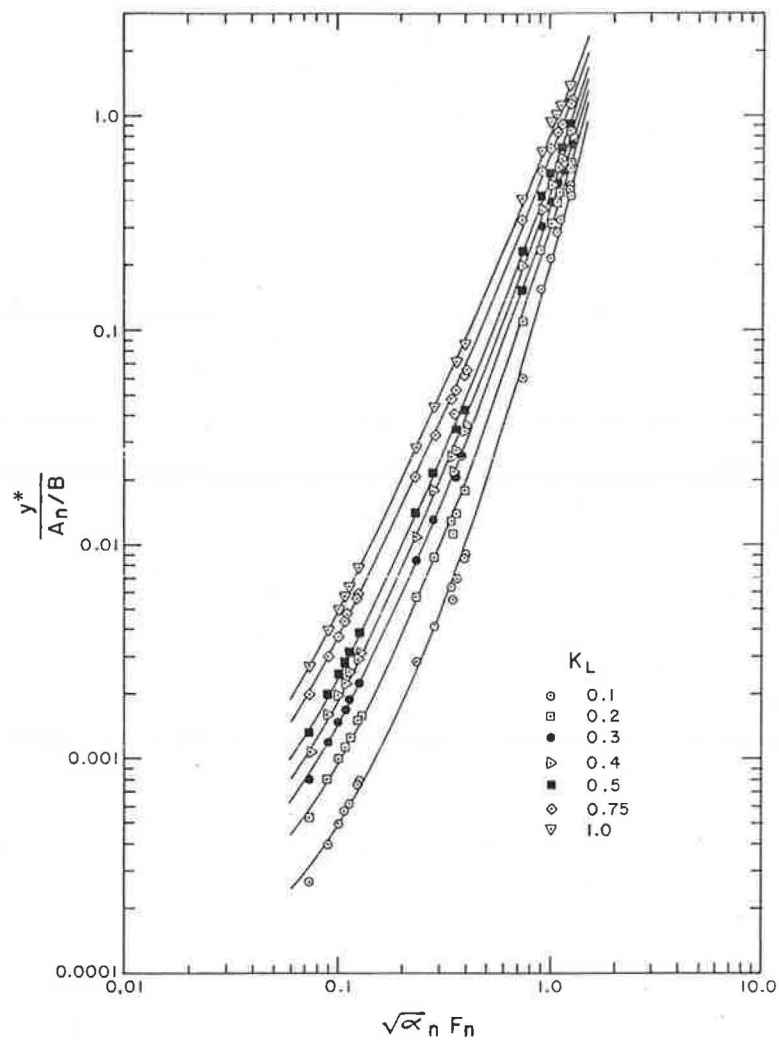


Figure 12. Change in water-surface elevation: case III, rigid boundary.

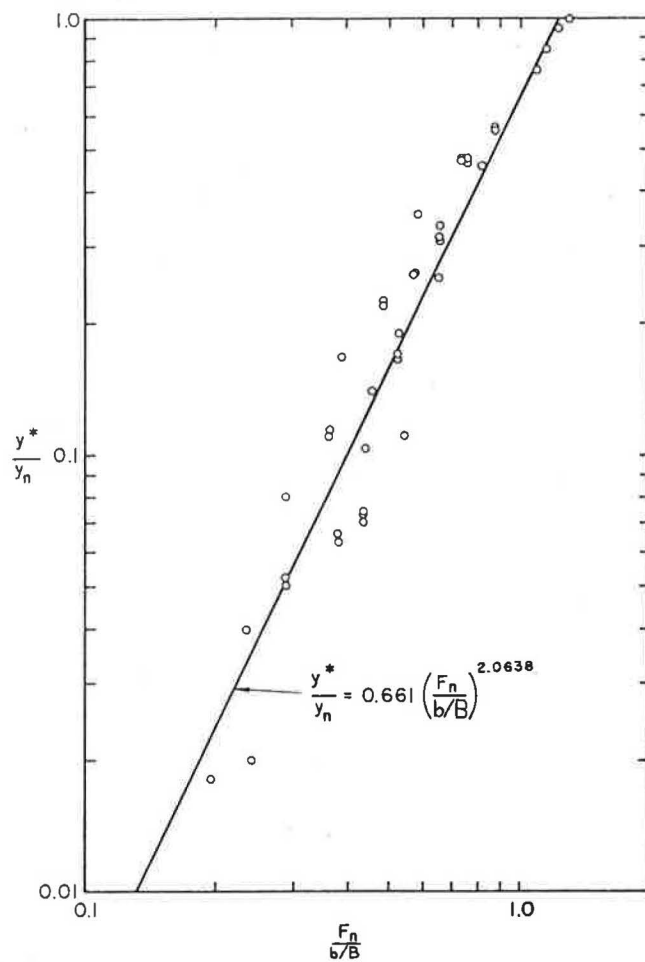
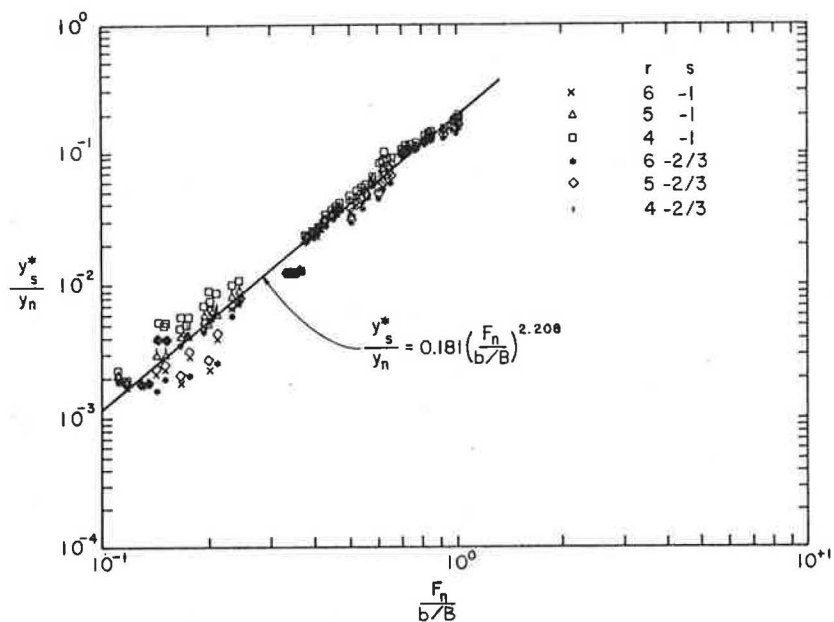


Figure 13. Change in water-surface elevation: case III, movable boundary.





to locate the appropriate backwater relations. Estimate the required nondimensional independent variables ( $F_n$ ,  $b/B$ ,  $K_{mc}/K$ ,  $n_{mc}/n_{ob}$ ,  $K_L$ ).

Step 3: Compute the backwater ratio  $y^*/y_1$  by assuming rigid-boundary hydraulics from the appropriate relation in Figure 9.

Step 4: Compute the constriction scour ratio  $\Delta y_s/y_1$ . If the bridge category is case I or case II, constriction scour is assumed to be negligible. For the remaining cases compute  $\Delta y_s/y_1$  as follows: case III, Equation 15; case IV, Equation 18; and case V, Equation 17.

Step 5: Compute the backwater ratio  $y_s^*/y_1$  by assuming movable boundary hydraulics from the appropriate relation in Figure 9.

Step 6: If the increase in stage ( $y^*$  or  $y_s^*$ , depending on whether the boundary is rigid or movable) is unacceptable, assume a new bridge opening and recompute  $y^*$  or  $y_s^*$ .

As with all regression-based equations, extrapolation outside the data range over which the equations were developed may give erroneous results.

## SUMMARY AND CONCLUSIONS

### Analysis of Backwater and Constriction Scour

Expressions for backwater based on the conservation of energy in open-channel flow were presented for five commonly occurring bridge crossings. To satisfy the one-dimensional flow assumption, the theories of potential flow and empirical results were used to locate cross sections in zones of nearly one-dimensional flow. An expression for constriction scour was derived as a function of the ratio of channel width to bridge opening width and exponents describing the bed-load transport rate. A procedure referred to as the known cross-section method was

Figure 14. Change in water-surface elevation: case IV, movable boundary.

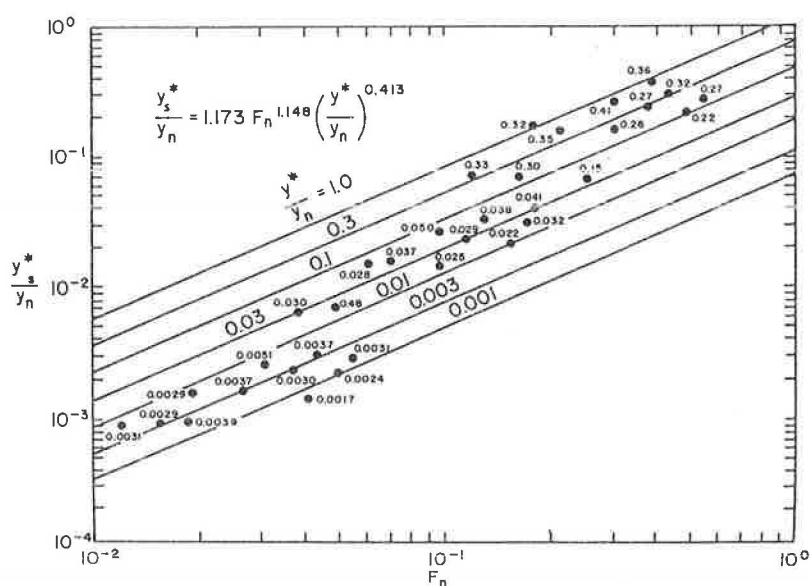


Figure 15. Change in water-surface elevation: case V, movable boundary.

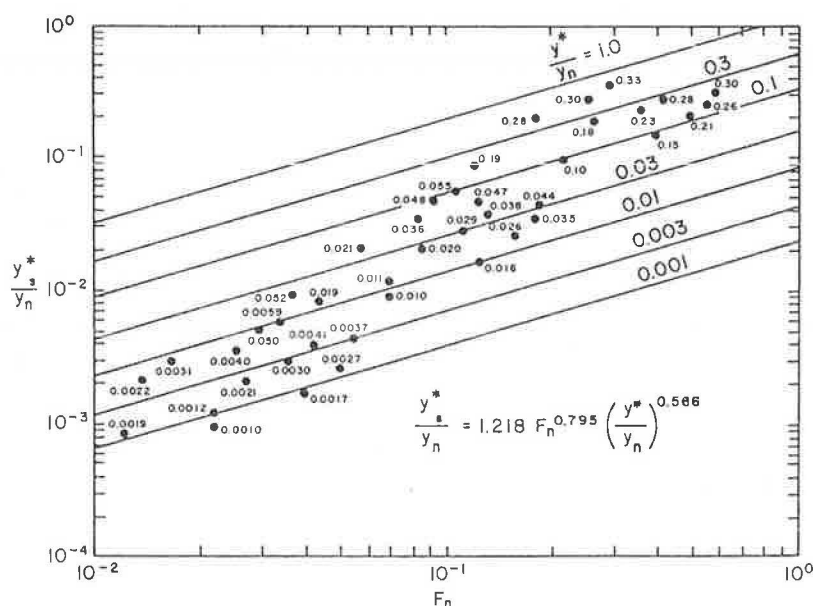


Figure 16. Comparison of changes in water-surface elevation for cases IV and V, rigid boundary.

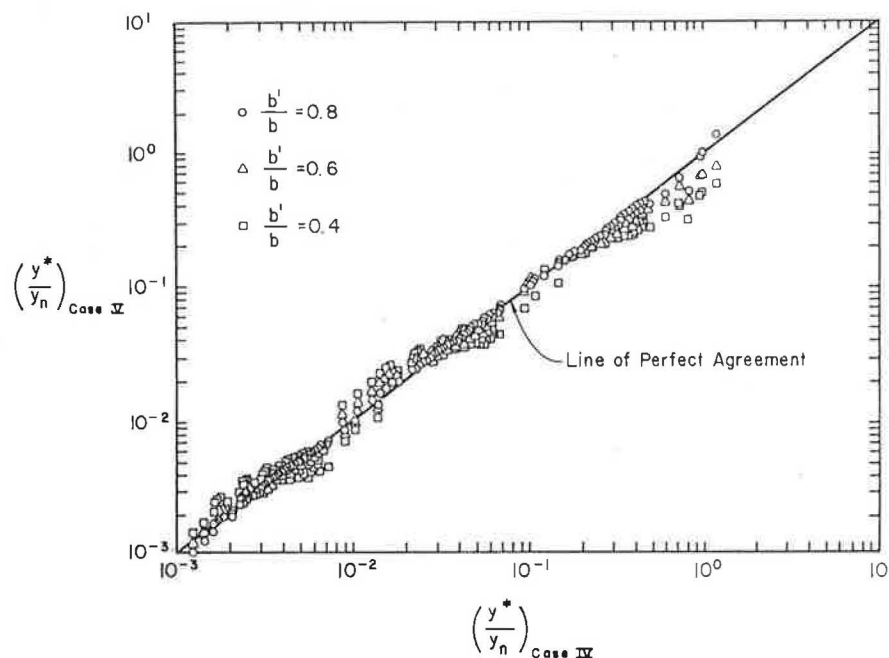


Figure 17. Range of data used in regression analysis.

Case	$y_n$ (ft)	$b$ (ft)	$b'$ (ft)	$B$ (ft)	$z'$ (ft)	$S_n$	$\eta_m$	$\eta_{oh}$	$Q(\text{ft}^3/\text{s})$	$K_f$	$F_n$
I	10-50	82-98	—	100	—	0.00001-0.005	0.030	—	640-150,000	0.1 -0.4	0.033-0.81
II	3-20	82-98	10-30	100	1-15	0.0001-0.01	0.030	0.01	69-15,200	0.1 -1.0	0.04-0.91
III Rigid	0.33-0.72	2-6	—	7.9	—	0.001-0.0012	0.022	—	2.5-5.0	—	0.065-0.29
III Movable	1-52	50-90	—	100	—	0.00014-0.0019	0.030	—	57-99,000	1.4 -3.0	0.1 -0.5
IV	12-80	50-250	50-250	1000	10-50	0.00001-0.001	0.030	0.075-0.15	490-590,000	0.077-2.9	0.12-0.59
V	12-80	62.5-625	50-250	1000	10-50	0.00001-0.001	0.030	0.075-0.15	490-590,000	0.13 -23	0.12-0.59

developed for easily assessing the effects of constriction scour on backwater.

#### Simple Methods for Estimating Backwater

Through numerical simulation, dimensional analysis, and regression analysis, explicit relations for bridge backwater were developed for both rigid- and movable-boundary conditions. For bridge piers, it was found that the backwater is a function of the Froude number, the kinetic-energy coefficient, and a pier energy-loss coefficient. The Froude number and the ratio of bridge opening width to channel width were found to describe the backwater in a channel abrupt encroachment. In the case of floodplain encroachments, the Froude number and the ratio of main channel conveyance to total conveyance were found to be the primary parameters controlling backwater. These solutions are of an accuracy suitable for use in a bridge feasibility or preliminary design study; the backwater regression equations, however, are not intended for detailed analyses.

#### Practical Application

Step-by-step procedures were given to demonstrate how the simple backwater and constriction scour relations may be applied to feasibility studies.

#### Recommendations

Further studies are necessary to quantify the multi-

dimensional flow phenomena resulting from floodplain encroachment. The time dependence of bridge scour and development of armor layers within the bridge waterway also need further investigation. Last, both analytic and simplified procedures need to be verified against field data.

#### REFERENCES

1. S.W. Taylor. Flow Modification by Bridges and Abrupt Encroachments. Department of Civil Engineering, Colorado State Univ., Fort Collins, Colo., M.S. thesis, 1982.
2. J.N. Bradley. Hydraulics of Bridge Waterways. FHWA, Hydraulic Design Series 1, 1978.
3. H.K. Liu, J.N. Bradley, and G.J. Plate. Backwater Effects of Piers and Abutments. Colorado State Univ., Fort Collins, Colo., Rept. CER57HKL10, 1957.
4. V.R. Schneider, J.W. Board, B.E. Colson, F.H. Lee, and L. Druffel. Computation of Backwater and Discharges at Width Constrictions of Heavily Vegetated Flood Plains. U.S. Geological Survey, Reston, Va., Water Resources Investigation 76-129, 1977.
5. D.E. Abbott and S.J. Kline. Experimental Investigation of Subsonic Turbulent Flow Over Single and Double Backward Facing Steps. ASME Journal of Basic Engineering, Series D, Vol. 84, 1962, pp. 317-325.

6. V.P. Lokrou. Characteristics of Flow in Channel Abrupt Expansions. Department of Civil Engineering, Colorado State Univ., Fort Collins, Colo., Ph.D. thesis, 1979.
7. E.M. Laursen and A. Toch. Scour Around Bridge Piers and Abutments. Iowa Highway Research Board, Bull. 4, May 1956, pp. 36-38.
8. H.W. Shen. Scour Near Piers. In River Mechanics (H.W. Shen, ed.), Volume 2, Chapter 23, Colorado State Univ., Fort Collins, Colo., 1971.
9. E.V. Richardson, D.B. Simons, S. Karaki, K. Mahmood, and M.A. Stevens. Highways in the River Environment: Hydraulic and Environmental Design Considerations. FHWA, Training and Design Manual, May 1975.
10. E.M. Laursen. The Application of Sediment Transport Mechanics to Stable Channel Design. Journal of the Hydraulics Division of ASCE, Vol. 82, No. HY4, 1956.
11. E.M. Laursen. Scour at Bridge Crossings. Journal of the Hydraulics Division of ASCE, Vol. 86, No. HY2, Proc. Paper 2369, Feb. 1960, pp. 39-54.
12. E.M. Laursen. The Total Sediment Load of Streams. Journal of the Hydraulics Division of ASCE, Vol. 84, No. HY1, Proc. Paper 1530, Feb. 1958, pp. 1530-1 through 1530-36.
13. V.T. Chow. Open-Channel Hydraulics. McGraw-Hill, New York, 1959.
14. H.H. Darnes. Roughness Characteristics of Natural Channels. U.S. Geological Survey, Reston, Va., Water-Supply Paper 1849, 1977.